ORIGINAL ARTICLE

Metabolic Matching and Morphofunctional Parameters of Deceased Donor Kidney Transplantation: A Study of Super-Rapid and Delayed Recovery in Asystole Donors

Ashimov Zhanybek[1], Mamakeev Kanat[1], Ashimov Isabek[2], Niyazov Batyrkhan[2], Akmatov Taalaibek[1], Yethindra Vityala[3]

[1]Department of Scientific, National Surgical Center Named after M.M. Mamakeev of the Ministry of Health of the Kyrgyz Republic, Bishkek, Kyrgyzstan, [2]Department of General Surgery, Kyrgyz State Medical Institute of Retraining and Advanced Training Named after S.B. Daniyarov, Bishkek, Kyrgyzstan, [3]Honorary International Faculty, AJ Research Centre, AJ Institute of Medical Sciences and Research Centre, Mangaluru, Karnataka, India

Abstract

Introduction: Deceased donor kidney transplantation is a crucial alternative for patients with end-stage renal disease lacking living donors. This study aimed to characterize the morphofunctional parameters of post-mortem renal allograft (RA ex-mortuo) transplantation when modeling super-rapid recovery and delayed recovery for two types of asystole donors. **Materials and Methods:** The study assessed the morphological and histochemical parameters of RA ex-mortuo under *ex vivo* conditions in 39 dogs. The morphological analysis involved kidney biopsies and perfusate examination using light microscopy, morphometric studies, and histostereometric analysis. The study evaluated the height of the renal epithelium in the proximal and distal tubules, the specific volume of glomeruli in the cortex, and the prevalence of dystrophic changes in the tubular epithelium. Lipid peroxidation products in the perfusate were analyzed, and tissue enzyme activity was measured. The study proposed an evaluation algorithm and corresponding criteria to characterize the resource potential of delayed recovery. The effectiveness of RA rehabilitation ex-mortuo was evaluated using a scale based on morphological and metabolic disorder severity. **Results:** The study pioneered the multicriteria principle to classify asystolic donors as super rapid and delayed recovery, enhancing the understanding of theoretical and practical integration in simulated reality. Using non-perfusion hypothermia *ex vivo* for rehabilitating RA ex-mortuo requires 60 min to lower basal metabolism, as indicated by reduced succinate dehydrogenase and phenoloxidase activity. Early rehabilitation stages showed decreased metabolism, with enzyme activity significantly decreasing at 30 min. Metabolic disorders were satisfactory at 35 points and mild to severe at 16 points. **Conclusion:** The activity of key enzymes during ex-mortuo RA rehabilitation showed reduced metabolic processes in both models. Indicators such as AR (−0.09) and AF (0.001%) suggest positive rehabilitation outcomes at both 30 and 120 min, which are closely linked to the temporal risk factor.

Key words: Asystole donor, deceased donor kidney transplantation, immunosuppression, metabolic matching, morphofunctional parameters, renal allograft

INTRODUCTION

Deceased donor kidney transplantation (DDKT) is crucial for renal allograft (RA) transplantation and offers an alternative for patients with end-stage renal disease lacking living donors. Fernando *et al*. reported a 75.8% 1-year recipient survival rate and a graft survival rate of 89.58% for DDKT, which can be enhanced by optimizing ischemia time and immunosuppression.[1] Xiong *et al*.

Address for correspondence:
Ashimov Zhanybek, Department of Scientific, National Surgical Center Named after M.M. Mamakeev of the Ministry of Health of the Kyrgyz Republic, Bishkek, Kyrgyzstan.
E-mail: ashimovzhanybeknsc@gmail.com

Received: 06-08-2024
Revised: 21-09-2024
Accepted: 29-09-2024

and Laging *et al*. found that DDKT, despite having lower graft survival rates than living-related kidney transplantation, results in higher long-term estimated glomerular filtration rates.[2,3] Donor age significantly affects graft survival, with an increased graft failure risk following a J-shaped curve for both living and deceased donors.[3]

Despite the lower graft survival rates in DDKT than in living donor kidney transplantation,[4] ABO-incompatible living donor kidney transplantation may yield better patient survival rates than waiting for an ABO-compatible deceased donor, particularly in regions with active ABO-incompatible living donor kidney transplantation programs and prolonged waiting times for DDKT. This underscores the complex interplay between donor type, compatibility, and regional transplantation practices.

Therefore, metabolic matching is essential for the success of post-mortem RA ex-mortuo transplantation. By understanding the metabolic status of RA ex-mortuo, clinicians can select medications that activate or suppress specific enzymes.[5,6] However, this concept remains under-recognized despite its scientific and practical significance.

Assessing the quality of RA ex-mortuo within an acceptable timeframe for transplantation (30–120 min) is a pressing clinical and theoretical task in modern transplantology. This study aimed to characterize the morphofunctional parameters of RA ex-mortuo transplantation when modeling super-rapid recovery and delayed recovery for two types of asystole donors, with organ recovery typically occurring within 30 min (super rapid recovery) and 60–120 min (delayed recovery) after controlled or uncontrolled donation after circulatory death, respectively.

MATERIALS AND METHODS

This study assessed the morphological and histochemical parameters of RA ex-mortuo under *ex vivo* conditions in 39 dogs, adhering to the international standards for humane treatment. The dogs received appropriate care, feeding, and anesthesia during the ex-mortuo explication of RA, and were humanely euthanized post-experiment.

The morphological analysis involved kidney biopsies and perfusate examination using conventional light microscopy. For morphometric studies, cortex and medulla samples were paraffin-embedded, sectioned, and stained with hematoxylin and eosin. Histostereometric analysis was performed using a screw eyepiece micrometer, a LOMO Biolam 70 compound microscope (LOMO, St. Petersburg, Russia) and an ocular planimetric technique. Measurements of glomeruli and capsule diameters in renal corpuscles were performed, and their volumes were calculated using the formula $V = \pi \times ab^2$, where a is the major axis and b is the minor axis. The volume ratio of glomeruli to capsules was determined using $\frac{Vglomerulus}{Vcapsules - Vglomerulus}$ and $P = Vglomerulus \times \frac{10}{Vcapsules}$. An increased P coefficient indicated a larger glomerulus volume, whereas a decreased coefficient suggested a larger capsule volume.

The study evaluated the height of the renal epithelium in the proximal and distal tubules and the specific volume of glomeruli in the cortex using a formula to calculate the prevalence of dystrophic changes in the tubular epithelium. Linear parameters of 30 renal corpuscles and tubules were also determined. Materials were obtained through kidney biopsy and samples of flowing blood and perfusate at 60–120 min. Lipid peroxidation products in the perfusate were analyzed by ultraviolet absorption of hexane extracts and tissue enzyme activity was measured. This study assessed RA ex-mortuo data on morpho-, ultrastructural, and histoenzymatic disorders along with lipid peroxidation-associated disorders. The rehabilitation potential of certain technologies was evaluated using quantitative and qualitative morphological and metabolism criteria. The study concluded that the proposed evaluation algorithm and corresponding criteria effectively characterized the resource potential of the delayed recovery [Table 1].

The effectiveness of RA ex-mortuo rehabilitation was evaluated using the following scale: (1) Satisfactory (4–5 points), (2) Weak (2–3 points), and (3) Negative (0–1 point). This method offers unified quantitative gradation for each criterion. The points for each criterion were summed to derive the final score (Σ). The final step involves comparing the potential of the automated control system with the actual control system to determine correspondence, with five points indicating full correspondence, three points indicating partial correspondence, and 0–1 points indicating no correspondence.

Table 1: Criteria for assessing the effectiveness of cold protection of RA ex-mortuo outside the body

Performance evaluation criteria		Points
1.	Severity of morphological disorders:	
	The morpho- and ultrastructure are well preserved;	5
	Mild disturbances of morpho- and ultrastructure;	3
	Severe disturbances of morpho- and ultrastructure.	3
2.	Changes in the severity of metabolic disorders:	
	Minor metabolic disorders;	5
	Moderate manifestations of metabolic disorders;	3
	Severe metabolic disorders.	1

RA: Renal allograft

This concept employs the delayed recovery category to identify new potential cadaveric donors with RA ex-mortuo. The multicriteria formulation stems from a hypothetical lack of information on morphofunctional disorders in the RA ex-mortuo parenchyma and their dynamics during rehabilitation. We pioneered the multicriteria principle to classify asystolic donors as super rapid and delayed recovery, enhancing the understanding of theoretical and practical integration in a simulated reality. The results were organized into a four-field contingency table to evaluate rehabilitation effectiveness, delayed, and super rapid recovery compliance [Table 2]. Calculations included the incidence (IN), relative risk (RR), attributable risk (AR), etiological fraction (EF), and odds ratio (OR).

This elucidates the use of various formulas to determine the relationship between the risk factors and rehabilitation outcomes of RA ex-mortuo. It begins by indicating that IN represents the frequency of positive and negative results in exposed $\left(RF+=\frac{a}{a}+b;2\right)$ and unexposed $(RF-=\frac{s}{s}+d)$ groups, contingent on the presence or absence of the studied factor. It then describes the calculation of RF+ and RF− and their application in computing RR = $\frac{RF+}{RF}$ which evaluates the correlation between risk factors and rehabilitation outcomes. In addition, it explains the computation of $AR=(RF+)-(RF-)$ or $RR=\frac{a}{(a+b)}-\frac{c}{(c+d)}$ and $EF=\frac{AR}{RF+}\times 100\%$, which excludes negative outcomes unrelated to a temporary risk factor. Finally, EF, representing the ratio of AR to IN in the exposed group (RF+), is typically expressed as a percentage.

The OR indicates how many times the chance of a negative result in the exposed group is greater than the chance in the unexposed group. Calculation using the following formula: OR = chance in the exposed group/chance in the non-exposed group or $OR=\frac{axb}{cxd}$. OR was assessed in the same way as RR: (1) OR=1 -indicates the absence of a connection between the factor being studied and the negative result of the rehabilitation of RA ex-mortuo; (2) OR>1 -there is a possible connection between a negative result and a temporary risk factor; (3) OR<1 -an assumption about the critical influence of the factor is possible.

Statistical analyses were performed using Statistical Packages for the Social Sciences version 11.5. Results are expressed as the mean ± standard deviation and n (%). $P < 0.05$ was considered as statistically significant at $P < 0.05$. This study was approved by the minutes of 2nd meeting of the bioethics committee of the National Surgical Center named after M.M. Mamakeev of the Ministry of Health of the Kyrgyz Republic (dated May 03, 2024) and was conducted in compliance with the criteria outlined in the declaration of Helsinki.

Table 2: Correlation between the results of assessing the effectiveness of rehabilitation of RA ex-mortuo and the compliance of super rapid and delayed recovery(in points)

Comparison groups	Rehabilitation and compliance effectiveness		Total
	+	-	
Super rapid recovery	a	b	a+b
Delayed recovery	c	d	c+d
Total	a+c	b+d	a+b+c+d=n

RA: Renal allograft

RESULTS

Micro- and ultrastructural examinations indicated that 30 min of non-perfusion cold rehabilitation did not alter the ultrastructure of endothelial cells in the renal parenchyma. However, at 60 min, ultramicroscopic disorders of the endothelium of the glomerular capillaries were observed. Electron diffraction patterns revealed enlarged endothelial cells with all layers of the glomerular filter visible, bulging nucleated zones into the capillary lumens, and uneven nuclear contours. After 30 min, granular chromatin components were concentrated around the nucleolus and near the karyolemma, and the cytoplasmic matrix in the perikaryon zone of endothelial cells was cleared, indicating submicroscopic changes in the hyaloplasm [Figure 1].

At 60 min, the basement membrane appeared less electron-dense, widened, loosened, or unevenly thickened compared with the control group. In the control group, the glomerular epithelium consisted of epithelial cells and podocytes adjacent to the basement membrane from the urinary space side, with a light and less electron-dense cytoplasm. After 30 min, hyaloplasm swelling was accompanied by organelle swelling, and pores were clearly visualized in the thinned cytoplasm of endothelial cells, extending to the peripheral

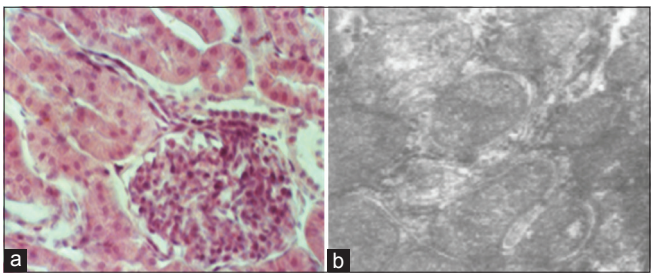

Figure 1: Super rapid recovery. (a) hematoxylin and eosin staining showing the structure of *ex vivo* dog RA after 30 min of non-perfusion preservation, showing the glomerulus and convoluted tubules of the renal cortex (×600); (b) electron micrograph of fine structure showing proximal tubule epithelial cells in an undamaged dog kidney, displaying intact mitochondria and reticulum cisterns (×20,000)

zone of the cells containing pores. At 60–90 min, podocyte nuclear contours were usually uneven and chromatin was loosely distributed in the cleared nucleoplasm or formed marginal clusters.

At 30 min, swollen mitochondria and branched granular endoplasmic reticulum with expanded channels forming cisterns were observed in the cytoplasm near the plasma membrane [Figure 2]. Electron diffraction patterns indicated structural disturbances in podocytes, with enlarged pedicles and merged pedicles disrupting the spatial organization of filtration slits. At 120 min, podocyte dystrophic processes intensified, showing a highly vacuolated cytoplasm, expanded endoplasmic reticulum, deformed cisterns, and visible fat droplets near the nuclei. The pedicles separated from the trabeculae filled the subpodocytic space, whereas the trabeculae disintegrated and lost connections with the cells. At 30 min, numerous vacuoles filled with electron-dense mitochondrial material and podocyte trabecular fragments were present in the lumen of the Shumlyansky-Bowman capsule. At 120 min, the ultrastructure of cells in the proximal nephron tubule explained their function in resorbing water, sodium, potassium, chlorides, amino acids, and fully reabsorbing filtered glucose and protein.

In this study, tissue samples collected at 30 min showed no changes in the proximal tubule nephrocyte structure. Ultrastructural alterations were minimal, involving slight basement membrane thickening and increased gaps between basal labyrinth folds. At 120 min, the basal mitochondria maintained their structure, with a granular, electron-dense matrix, and numerous parallel cristae. However, some mitochondria showed a reduced matrix density and partially expanded cristae. Within 30 min, the epithelial cell cytoplasm in the convoluted region became clearer and more vacuolated, with chromatin clumping at the nuclear margins. At 60 min, the intercellular spaces expanded further and the proximal cells showed more damage. The basal folds of nephrocytes were significantly disordered due to reduced cytoplasmic invagination depth and increased space between the folds.

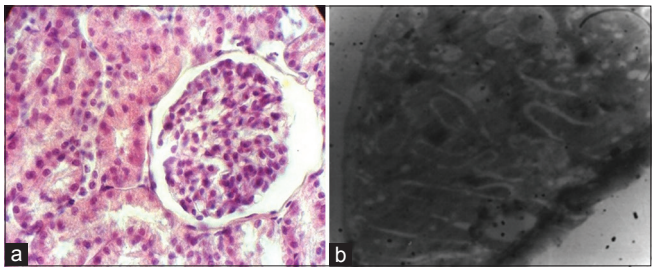

Figure 2: Delayed recovery. (a) hematoxylin and eosin-stained histological examination shows structural changes in the RA after 120 min of hypothermic non-perfusion. The renal cortex displays granular and fatty degeneration of the convoluted tubules (×600 magnification). (b) electron microscopy of the dog kidney cortex 120 min post-hypothermia revealed swollen nephrocyte mitochondria with disrupted cristae (×7000 magnification)

Within 30 min of observation, the cell cytoplasm was lightened due to vacuole formation between mitochondria, with mostly destroyed cristae. Electron diffraction patterns revealed a disrupted ultrastructural organization in the apical cell regions, marked by the loss of ordered microvilli, collapse, and desquamation. After 90–120 min, changes in apical plasma membrane geometry were accompanied by numerous primary and secondary lysosomes. Nephrocyte nuclei showed destruction, indicated by an expanded perinuclear space, marginal chromatin distribution, and smooth nucleoli contours. Some nuclei formed vacuoles next to the expanded perinuclear space within 30 min. The electron density of the nephrocyte hyaloplasm is slightly reduced. In addition, after 120 min, degenerative processes in the proximal tubules of dog kidneys were marked by small, intense eosin-stained grains.

After 30 min, the nephrocyte ultrastructures exhibited dilated and deformed endoplasmic reticulum cisterns, numerous cytoplasmic lysosomes, and disrupted metabolic processes. The cell nuclei displayed alterations in shape, chromatin organization, karyoplasm, and karyolemma. After 120 min, impaired nuclear membrane permeability was indicated by an expanded perinuclear space forming uneven light stripes, perinuclear vacuoles, and nucleoplasm clearing. The enlarged nucleus assumed unusual shapes with jagged edges and uneven chromatin distribution in the clumps. At 30 min, the apical section of the proximal cells showed ultrastructural changes, including swollen, widened, and electron density-reduced brush borders. After 120 min, the microvilli moved closer, with flask-shaped swellings at their ends and an increased presence of pinocytotic vacuoles and lysosomes in the apical cytoplasm.

Within 30 min of cooling, distal nephrons showed less pronounced epithelial reactions than proximal tubules, with no structural changes visible under light microscopy. However, ultrastructural changes were observed, including basement membrane loosening, uneven electron density, swollen mitochondria with clear matrices, some enlarged or with shortened cristae, and others partially fragmented or destroyed. After 60 min, more significant ultrastructural changes in the distal nephron were noted, such as lighter cytoplasm due to expanded endoplasmic reticulum cisterns and basal plasma fold spaces. Perinuclear space expansion and marginal chromatin distribution, with occasional shallow nuclear envelope invaginations into the karyoplasm, were also observed. After 120 min, histological preparations revealed protein and fatty degeneration in the distal tubules, with fat droplets occupying most of the cytoplasm. Ultrastructural changes intensified, with deepening and loosening of the basal plasma membrane outgrowths and folds, expanded basal labyrinth folds, and swollen mitochondria with partially or completely demolished cristae in some nephrocytes.

After 30 min, the nephron cytoplasm appeared vacuolated with single-membraned cytosomes, and the proximal nephron cells contained numerous lysosomes. Nephrocyte nuclei exhibit deformed and lobed contours. At 120 min, chromatin was redistributed near the inner layer of the nuclear membrane, clearing the nucleoplasm and expanding the perinuclear space. The nephron tubular system was more sensitive to cooling than the renal glomerulus within 30 min, with distal nephron epithelial reactions being less pronounced than proximal reactions. Morphological and ultrastructural changes varied in timing among the nephron elements. Preventive external hypothermia did not significantly alter the renal parenchyma at the light optical level within 30 min. However, after 60 min, ischemic changes deepened, with cell destruction, increased endothelial cell volume, nuclear alterations, and swelling of the hyaloplasm and organelles. After 120 min, the changes intensified, exhibiting intracellular edema, cytoplasmic vacuolization, early fatty degeneration, and mitochondrial structural disturbances.

The histoenzymatic study of RA ex-mortuo indicated increased enzyme activity at 30 min, which was likely due to gradual cooling. At 60 min, enzyme activity decreased to moderate levels (+). At 120 min, enzyme activity was weak (+), reflecting reduced cellular metabolism due to hypothermia. During non-perfusion hypothermia in RA ex-mortuo nephron cells, metabolism may proceed through low-level anaerobic oxidation, leading to the accumulation of cytotoxic metabolic products that impair cell function and structure. At 30 min, lactate dehydrogenase (LDH) activity was reduced sevenfold compared to normal, at 41 ± 10.63 mmoL/L ($P < 0.001$), suggesting a significant enzyme imbalance within the 1st 1/2-h due to the sudden cessation of oxygen, oxidation substrates, energy metabolites, and plastic metabolism, despite reduced oxygen demand from hypothermic protection [Table 3].

Table 3: Dynamics of enzyme activity in models of super rapid recovery and delayed recovery

Super rapid recovery			
Enzymes	**Control**	**5 min**	**30 min**
Lactate dehydrogenase	284.3±38.96	83±0.16*	62.6±0.15*
Acid phosphatase	0.16±0.02	0.32±0.02*	0.18±0.04
Alkaline phosphatase	0.95±0.13	0.47±0.11*	0.33±0.13*
Delayed recovery			
Enzymes	**Control**	**60 min**	**120 min**
Lactate dehydrogenase	284.3±38.96	68.6±0.18*	65.0±0.17*
Acid phosphatase	0.16±0.02	0.20±0.06	0.15±0.04
Alkaline phosphatase	284.3±38.96	68.6±0.18*	65.0±0.17*

min: Minutes. Values are expressed as mean±standard deviation. *$P<0.05$

Enzyme activity increased threefold at 60 min compared to the control group but remained 2.5 times lower than the LDH standard value of 122.6 ± 46.5 mmoL/L ($P < 0.01$). At 120 min, LDH activity further increased but stayed below the normal range at 164.64 ± 64.64 mmoL/L ($P > 0.05$). This slight increase in enzyme activity suggests a shift in RA metabolism under acute cold ischemia and possible disruption in cell membrane permeability, releasing membrane-bound enzymes into the perfusate.

Oxidoreductase activity decreased threefold at 30 min compared to the standard, reaching 0.054 ± 0.021 mmoL/L ($P < 0.002$), and continued to decline at 60–120 min to the minimum value of lysosomal enzyme acid phosphatase and brush enzyme rims of alkaline phosphate. At 60 min, acid phosphatase activity was still 3.5 times lower than the standard at 0.045 ± 0.026 mmoL/L ($P < 0.003$; $P1 > 0.05$). After 120 min, acid phosphataseactivity was reduced 4.5 times compared to the control, at 0.034 ± 0.017 mmoL/L ($P < 0.001$; $P1 > 0.05$; $P2 > 0.05$). Similar trends were observed for alkaline phosphatase (ALP) values.

Studies indicate that ALP activity decreased 4.5 times from the standard level to 0.214 ± 0.08 mmoL/L after 30 min of preservation ($P < 0.001$). After 60 min, ALP activity reduced 5.5 times to 0.17 ± 0.08 mmoL/L ($P < 0.05$), and by 120 min, it decreased 12 times to 0.08 ± 0.04 mmoL/L ($P < 0.001$; $P1 < 0.05$; $P2 < 0.05$). These findings suggest that the dynamics of ALP enzyme activity reflect the structural integrity of lysosomes and the brush border epithelium of the nephron tubules due to the protective effect of hypothermia.

At 30 min, LDH and oxidoreductase activities were halved compared to the control, showing weak activity (+) in the epithelium and glomerulus cells of the proximal and distal tubules. From 60 to 120 min, the activity of these enzymes was minimal (− +).

DISCUSSION

Deng *et al*. discussed the IN of glomerulonephritis in both living-related and deceased donor kidney transplants and noted its potential impact on metabolic status through renal function.[7]

However, several studies have addressed factors related to delayed graft function (DGF), a form of delayed recovery in DDKT. For instance, Park et al. identifies acute kidney injury,[12] continuous renal replacement therapy, smoking, and donor hypertension as independent risk factors for DGF in DDKT recipients.

Kaufmann et al. and Van Rijt et al. discussed the association of a single-nucleotide polymorphism in the erythropoietin gene with DGF and graft survival.[13,14] Saidi et al. provided insights into the outcomes of DDKT in older recipients, and noted comparable DGF rates among different age groups.[15] Van Rijt *et al*. investigated the role of erythropoietin levels and genetic polymorphisms in DDKT, highlighting the implications for the metabolic status of erythropoietin in erythropoiesis and cytoprotection.[14] Interestingly, while these studies focused on DGF, none specifically modeled super-rapid recovery post-transplantation. Moreover, the studies do not contradict each other but rather complement the understanding of various factors influencing DGF.

The duration of warm ischemia and the recovery process affect the morphofunctional characteristics of post-mortem RAs from non-heart-beating donors (NHBDs). Super-rapid recovery techniques aim to reduce ischemic time, whereas delayed recovery involves extended periods before preservation. Research has shown that despite longer warm ischemia times, NHBD kidneys do not necessarily exhibit increased vulnerability to allograft fibrosis.[12] *In situ* cooling methods and hyperosmolar citrate perfusion can mitigate warm ischemic effects, resulting in long-term function comparable to that of heart-beating donor kidneys.[13]

However, some studies have indicated that NHBD kidneys have higher rates of primary non-function and DGF than brain-dead heart-beating donor kidneys.[14] This suggests that ischemic injury may compromise morphofunctional integrity. Donor age also affects graft survival, with kidneys from older donors showing less favorable outcomes, particularly in heavier recipients.[15]

While NHBD kidneys are prone to ischemic injury, causing DGF, appropriate recovery techniques can maintain morphofunctional parameters, resulting in acceptable allograft survival rates.[12,13] This contradiction arises from varying degrees of ischemic injury affecting immediate graft function, which is a critical consideration in NHBD kidneys.[15] Therefore, meticulous donor selection and optimization of recovery protocols are essential for successful renal transplantation in NHBDs.

CONCLUSION

Using non-perfusion hypothermia *ex vivo* for rehabilitating RA ex-mortuo requires 60 min to lower basal metabolism, as indicated by reduced LDH and oxidoreductase activity. Early rehabilitation stages showed decreased metabolism, with enzyme activity significantly decreasing at 30 min. Metabolic disorders were satisfactory at 35 points and mild to severe at 16 points. The activity of key enzymes during RA ex-mortuo rehabilitation showed reduced metabolic processes in both models. Indicators such as AR (−0.09) and EF (0.001%) suggest positive rehabilitation outcomes at both 30 and 120 min, which are closely linked to the temporal risk factor.

ACKNOWLEDGMENT

None.

REFERENCES

1. Fernando M, Surendran S, Thirumavalavan S, Kumar P, Noor Mohamed SK. Graft function and outcomes of deceased donor kidney transplant patients in a tertiary care center. Indian J Transpl 2019;13:179.
2. Xiong Y, Jiang J, Zhang H, Fu Q, Deng R, Li J, *et al*. Higher renal allograft function in deceased-donor kidney transplantation rather than in living-related kidney transplantation. Transplant Proc 2018;50:2412-5.
3. Laging M, Kal-van Gestel JA, van de Wetering J, Ijzermans JN, Weimar W, Roodnat JI. The relative importance of donor age in deceased and living donor kidney transplantation. Transpl Int 2012;25:1150-7.
4. Koo TY, Lee J, Lee Y, Kim HW, Kim BS, Huh KH, *et al*. Outcomes of ABO-incompatible living donor kidney transplantation compared to waiting or deceased donor kidney transplantation. Am J Nephrol 2024;55:235-44.
5. Guibert EE, Petrenko AY, Balaban CL, Somov AY, Rodriguez JV, Fuller BJ. Organ preservation: Current concepts and new strategies for the next decade. Transfus Med Hemother 2011;38:125-42.
6. Fabre E, Conti M, Paradis V, Droupy S, Bedossa P, Legrand A, *et al*. Impact of different combined preservation modalities on warm ischemic kidneys: Effect on oxidative stress, hydrostatic perfusion characteristics and tissue damage. Urol Res 2002;30:89-96.
7. Deng R, Dai Y, Zhang H, Liu L, Li J, Xiong Y, *et al*. Higher incidence of renal allograft glomerulonephritis in living-related donor kidney transplantation. Transplant Proc 2018;50:2421-5.
8. Bains JC, Sandford RM, Brook NR, Hosgood SA, Lewis GR, Nicholson ML. Comparison of renal allograft fibrosis after transplantation from heart-beating and non-heart-beating donors. Br J Surg 2005;92:113-8.
9. Kimber RM, Metcalfe MS, White SA, Nicholson ML. Use of non-heart-beating donors in renal transplantation. Postgrad Med J 2001;77:681-5.
10. Medina-Polo J, De La Rosa F, Pamplona M, Rodríguez A, Villacampa F, Passas J, *et al*. MP-06.13 A comparison of the outcomes of renal transplantation from heart-beating cadaveric donors and non-heart-beating who present irreversible cardiac arrest occurring outside the hospital. Urology 2011;78:S72.
11. Mizutani K, Kinukawa T, OnoY, Ohshima S, Fujita T. Outcome of kidneys from older donors in

non-heart-beating cadaveric transplantation and their effective use. Transplantation 1999;67:S582.
12. Park WY, Kim Y, Paek JH, Jin K, Roh YN, Park UJ, *et al*. Impact of donor factors on post-transplant delayed recovery of graft function in deceased donor kidney transplantation. Korean J Transplant 2020;34:S98.
13. Kaufmann KB, Baar W, Silbach K, Knörlein J, Jänigen B, Kalbhenn J, *et al*. Modifiable risk factors for delayed graft function after deceased donor kidney transplantation. Prog Transplant 2019;29:269-74.
14. Van Rijt WG, Damman J, Snieder H, Seelen M, Van Goor H, Navis G, *et al*. Functional EPO gene polymorphism rs1617640 affects graft survival after deceased donor kidney transplantation. Transplant Immunol 2014;31:228.
15. Saidi RF, Kennealey PT, Elias N, Kawai T, Hertl M, Farrell M, *et al*. Deceased donor kidney transplantation in elderly patients: Is there a difference in outcomes? Transplant Proc 2008;40:3413-7.

Source of Support: Nil. **Conflicts of Interest:** None declared.